Dig Dis Sci (2015) 60:2963–2975
DOI 10.1007/s10620-015-3698-5

ORIGINAL ARTICLE

Role of Dopamine and D2 Dopamine Receptor in the Pathogenesis of Inflammatory Bowel Disease

Ganna Tolstanova[1,2] · Xiaoming Deng[1] · Amrita Ahluwalia[1] · Brankica Paunovic[1] · Alona Prysiazhniuk[2] · Lyudmyla Ostapchenko[2] · Andrzej Tarnawski[1] · Zsuzsanna Sandor[1] · Sandor Szabo[1]

Received: 11 February 2015 / Accepted: 29 April 2015 / Published online: 14 May 2015

Abstract
Background VEGF-induced vascular permeability and blood vessels remodeling are key features of inflammatory bowel disease (IBD) pathogenesis. Dopamine through D2 receptor (D2R) inhibits VEGF/VPF-mediated vascular permeability and angiogenesis in tumor models. In this study, we tested the hypothesis that pathogenesis of IBD is characterized by the disturbance of dopaminergic system and D2R activity.
Methods IL-10 knockout (KO) mice and rats with iodoacetamide-induced ulcerative colitis (UC) were treated intragastrically with D2R agonists quinpirole (1 mg/100 g) or cabergoline (1 or 5 μg/100 g). Macroscopic, histologic, and clinical features of IBD, colonic vascular permeability, and angiogenesis were examined.
Results Although colonic D2R protein increased, levels of tyrosine hydroxylase and dopamine transporter DAT decreased in both models of IBD. Treatment with quinpirole decreased the size of colonic lesions in rats with iodoacetamide-induced UC ($p < 0.01$) and reduced colon wet weight in IL-10 KO mice ($p < 0.05$). Quinpirole decreased colonic vascular permeability ($p < 0.001$) via downregulation of c-Src and Akt phosphorylation. Cabergoline (5 μg/100 g) reduced vascular permeability but did not affect angiogenesis and improved signs of iodoacetamide-induced UC in rats ($p < 0.05$).
Conclusions Treatment with D2R agonists decreased the severity of UC in two animal models, in part, by attenuation of enhanced vascular permeability and prevention of excessive vascular leakage. Hence, the impairment dopaminergic system seems to be a feature of IBD pathogenesis.

Keywords Inflammatory bowel disease · Animal models · Dopamine · D2 dopamine receptor · Vascular permeability

✉ Sandor Szabo
sszabo@uci.edu

Ganna Tolstanova
gtolstanova@gmail.com

[1] VA Long Beach Healthcare System, Departments of Medicine, Pathology and Pharmacology, VA Medical Center (05/113), University of California-Irvine, 5901 East 7th Street, Long Beach, CA 90822, USA

[2] Educational-Scientific Center "Institute of Biology", Taras Shevchenko National University of Kyiv, Kiev, Ukraine

Introduction

Inflammatory bowel diseases (IBD)—Crohn's disease (CD) and ulcerative colitis (UC)—are chronic debilitating gastrointestinal disorders that markedly impair quality of life and account for substantial costs to the healthcare system and society [1, 2]. IBD may develop at any age, often resulting in increased susceptibility to colorectal cancer and mortality [2, 3].

Extensive experimental and clinical studies confirmed the important role of pathologic angiogenesis with malformed, leaky vessels in the pathogenesis of IBD, especially in its chronicity [4–10]. We and others showed that vascular endothelial growth factor, also known as vascular permeability factor (VEGF/VPF), plays a central role in the initiation and perpetuation of abnormal vascular changes during IBD [11–14]. Moreover, VEGF was recommended as an additional vascular marker into a diagnostic algorithm for improved accuracy of IBD identification and differentiation of CD from UC [15]. We reported for the first time that diminished VEGF/VPF bioavailability by

neutralizing antibody to VEGF significantly ameliorates experimental UC in rats by preventing excessive vascular permeability and decreasing inflammatory cells infiltration via VEGF–VEGF receptor 2 (VEGFR2)-Src-dependent mechanism [11]. Recently, treatment with bevacizumab, a humanized IgG1 monoclonal antibody to VEGF, showed promising results in patients with IBD [16].

Despite positive experimental and clinical data on the inhibition of VEGF-induced pathologic angiogenesis in IBD treatment, high cost of neutralizing antibody [17] and non-specificity of anti-angiogenic multikinase inhibitors [18] encourage the search for inexpensive and more specific targets. Dopamine strongly and selectively inhibits vascular permeability and angiogenic action of VEGF/VPF in mouse models of ovarian tumor, human breast, and colon cancer with concomitant inhibition of tumor growth [19, 20]. VEGFR2 phosphorylation, which is critical for promoting angiogenesis and vascular permeability, is significantly enhanced in tumor endothelial cells collected from the dopamine-depleted and D2R knockout mice [21]. Dopamine prevented VEGF/VPF-induced vascular permeability via inhibition of VEGFR2-Src intracellular pathway [22] and stabilized tumor blood vessels via D2R-dependent upregulation of angiopoietin 1 (Ang1) in pericytes and the zinc finger transcription factor, Krüppel-like factor 2 (KLF2), in tumor endothelial cells [23]. Impaired synthesis of dopamine was demonstrated in inflamed mucosa of CD and UC patients [24] as well as in colonic mucosa of TNBS-treated rats [25]. D2R TaqIA polymorphism, which confers a decreased receptor density, was associated with refractory CD [26].

However, little is known about the mechanistic role of dopamine/D2R in the pathogenesis of IBD. In the present study, we tested the hypothesis that dopaminergic system is an important protective factor in IBD by controlling enhanced vascular permeability and excessive vascular leakage via D2R and might be a potential target for IBD treatment. To study the pattern of dopaminergic system in IBD pathogenesis, we examined the role of D2R in two animal models of IBD—iodoacetamide-induced UC in rats as a model of acute and chronic UC with signs of chronic inflammation (increased angiogenesis, tissue remodeling, etc.) at the late time points (7 and 14 days) and spontaneously developing colitis in IL-10 KO mice as a model of chronic IBD.

Methods

Animals

Female Sprague–Dawley rats (170–200 g) (Harlan Laboratory, San Diego, CA), female Wistar rats (170–220 g) (Animal Research Facility, KNU, Kiev, Ukraine), and IL-10 knockout (KO) mice on a C57BL/6J background (12 weeks old), sex- and age-matched wild type C57BL/6J (Jackson Laboratory, Bar Harbor, ME), were used for these experiments. These studies were approved by the Subcommittee for Animal Studies of the R&D Committee of the VA Medical Center in Long Beach, CA, USA (protocol # 0710-580), and by the Institutional Animal Care and Use Committee of Taras Shevchenko National University of Kyiv, Ukraine (protocol # 0109U005336). Animals were housed in the animal research facility under standard environmental conditions (12:12-h light–dark cycle starting at 6 a.m.; temperature 21–23 °C; humidity 30–35 %). All animals had unlimited access to Purina chow and tap water. Rats and mice were euthanized by CO_2 inhalation with subsequent cervical dislocation according to the guidelines of the Institutional Animal Care and Use Committee.

Drugs and Reagents

Iodoacetamide, methylcellulose, hexadecyltrimethylammonium bromide, *o*-dianisidine hydrochloride, myeloperoxidase (MPO), Evans blue, fluorescein isothiocyanate-conjugated (FITC)–dextran, protease inhibitor cocktail, and other general chemicals of analytical grade were obtained from Sigma (St. Louis, MO). Phosphatase inhibitors were from Thermo Fisher Scientific Inc. (Waltham, MA). Tyrosine hydroxylase (TH) (#2792), Akt (#9272), phospho-Akt^{Ser473} (#S473), Src (#2123), phospho-Src family^{Tyr416} (#2101) antibodies for immunoblotting were from Cell Signaling Technology, Inc. (Danvers, MA). Dopamine transporter DAT (sc-14002) and D2-R (sc-5305) and β-actin (sc-47778) antibodies for immunoblotting or immunohistochemistry were from Santa Cruz Biotech. (Santa Cruz, CA). GAPDH antibody was obtained from EnCor Biotech. (Alachua, FL). Anti-Von Willebrand factor antibody for immunohistochemistry was obtained from Chemicon Int. (Temecula, CA). Rubber catheter Nelaton S-8 was from Rüsch (Germany). D2R agonists (−)—quinpirole hydrochloride (quinpirole) and cabergoline (Dostinex) were obtained from Sigma (St. Louis, MO) and Pfizer (Kent, NJ), respectively.

Iodoacetamide-Induced UC Model

Experimental UC was induced in rats by the sulfhydryl alkylator iodoacetamide. A single dose of 6 % iodoacetamide is sufficient to induce well-reproducible colonic lesions, with the initial manifestations (e.g., increased vascular permeability, massive mucosal edema) seen in 1–2 h after iodoacetamide enema, leading to erosions and ulcers (6–12 h), followed by extensive acute and chronic inflammation (7–14 days) [27]. Briefly, 0.1 ml of 6 %

iodoacetamide dissolved in 1 % methylcellulose or the vehicle 1 % methylcellulose was given once by enema (7 cm from anus) with rubber catheter Nelaton S-8 fitted to 1-ml syringe. Rats were euthanized 0.5, 1, 2, 6, 24 h, 7 and 14 days after intracolonic administration of iodoacetamide. At autopsy, 7 cm of distal colon was removed.

Clinical and Macroscopic Evaluation of UC

A combinatorial disease activity index (DAI), ranging from 0 to 9, was calculated by summation of score (0–3) for each of the following parameters: lethargy, diarrhea, and weight loss (Table 1). These parameters were assessed on the first, third, fifth and seventh day of experiment. For standardization procedure of macroscopic colonic lesions evaluation and prevention of bias through our study, each animal was weighted immediately before autopsy; at autopsy, the 7 cm of distal colon from anus was removed, opened longitudinally, rinsed with saline, gently blotted with filter paper, and weighted. Macroscopic colonic lesions (the colonic lesion areas (mm^2), colonic dilatation (mm), and colon wet weights (g/100 g body weight)) were assessed as described [27]. All experiments were repeated at least two times, and data were pooled.

Histologic Evaluation of Colonic Lesions

To assess histologic damage, full-thickness colonic tissue samples were fixed in 10 % buffered formalin, embedded in paraffin, sectioned (5-µm-thick sections), and stained with hematoxylin and eosin. Histologic slides were coded and examined by experienced pathologist who was unaware of the treatment. Histologic analysis of colon section from IL-10 KO mice for chronic active inflammation (mild, moderate, severe), cryptitis (yes, no), crypt abscesses (no, rare, focal), erosions (yes, no), and ulcers (yes, no) were performed [14]. The histologic evaluation of rat colon with iodoacetamide UC was done according to the scoring system described previously [27].

Myeloperoxidase (MPO) Activity in the Colon

Neutrophil infiltration in the colon was quantified by measuring of MPO activity, as described earlier [28]. Briefly, about 50 mg of colonic tissue was homogenized in 1 ml of 50 mM phosphate buffer (pH 6.0) containing 0.5 % hexadecyltrimethylammonium bromide on ice. The homogenate was sonicated for 10 s, freeze-thawed three times, and centrifuged at 14,000 rpm for 15 min (4 °C). The supernatant (14 µl) was added to the reaction buffer (1 mg/ml of *o*-dianisidine hydrochloride and 0.0005 % hydrogen peroxide), and the activity of MPO was measured at 460 nm using serially diluted MPO (0.5, 0.25, 0.125, 0.06, 0.03, and 0.015 U/ml) as standard. The results were expressed as MPO activity U/gram of tissue.

In Vivo Measurement of Vascular Permeability

For quantitative studies of colonic vascular permeability, we used Evans blue that binds to albumin and its leakage reflects the increased vascular permeability of macromolecules [29]. Rats were anesthetized by inhalation of isoflurane, and Evans blue (0.4 mg/100 g in PBS) was injected intravenously 15 min before autopsy; rats were killed at 0.5 and 1 h after 6 % iodoacetamide enema or vehicle, 1 % methylcellulose. The abdomen was opened; 7 cm of colon was removed, rinsed in saline, gently blotted with filter paper, and weighed. Evans blue was extracted from the tissue using chloroform and measured by spectrophotometry at 610 nm. Results were expressed as mg dye/g wet weight colon.

In Vivo Measurement of Epithelial Permeability

To measure colonic epithelial permeability, we used blood concentration of FITC–dextran (MW 3.0–5.0 kDa) administered by gavage 20 ml/kg of PBS (pH 7.4) containing 22 mg/ml FITC–dextran 2 h before autopsy as described previously [30]. Plasma (100 µl) concentration of fluorescein was measured using a microplate spectrofluorimeter

Table 1 Disease activity index (DAI) score

Score	% Weight loss	Diarrhea	Lethargy
0	None	Normal droppings	Lively/normal
1	1–10	Soft or watery stool resulting in discoloration of a small ($\leq$1 cm^2) area near the anus	Mildly raised hair and dirtiness
2	11–15	Yellowish color of the abdominal hair involving >1 cm^2 are near anus	Dirtiness and decreased spontaneous movements
3	>15	Discoloration of abdomen extending to the chest	Barely moving and "neglected" animal

(NovoStar, BMG LABTECH Inc., Durham, NC) with excitation wavelength of 485 nm and an emission wavelength of 520 nm using serially diluted samples of the marker as standard.

Western Blot

At autopsy, the removed colon was cut along anti-mesenteric side and thoroughly rinsed in cold PBS. Colon was gently wiped by paper towel and flat by mucosa side up on ice. Using metal spatula, we gently scraped mucosa from the muscular layer. Total proteins (50, 100, or 150 μg) extracted from colonic mucosa in a lysis buffer containing protease and phosphatase inhibitors were processed routinely for Western blot as described previously [31]. The primary antibodies were used against tyrosine hydroxylase (TH) (1:1000), Akt (1:500), phospho-Akt^{Ser473} (1:500), Src (1:1000), phospho-Src family^{Tyr416} (1:750), dopamine transporter DAT (1:250), and D2-R (1:250). The loading controls were performed using a mouse monoclonal antibody to GAPDH (1:2000) or β-actin (1:500). Each Western blot was repeated at least two times.

Immunohistochemistry

Immunostaining was performed using paraffin-embedded 5-μm-thick intestinal sections. Sections were deparaffinized, hydrated, blocked for endogenous peroxidase using 3 % H_2O_2/H_2O, and subsequently subjected to microwave antigen retrieval using a Dako target retrieval solution (BD PharMingen, CA) at pH 10.00. Overnight incubation at 4 °C was performed with primary antibodies: rabbit polyclonal anti-Von Willebrand factor (1:100) or rabbit polyclonal DAT (1:200), followed by biotinylated secondary antibodies and a peroxidase-labelled streptavidin–biotin staining technique, and then the ABC detection method was performed using a Nikon microscope. To ensure the specificity of the antibody, immunoabsorption of the antibodies was performed to provide controls.

Morphometric Analysis of Colonic Microvasculature

Computerized morphometric analysis was performed using a standardized method for quantification of angiogenesis. Briefly, immunostained colonic sections with anti-Von Willebrand factor were examined under a Nikon microscope at low power (40×) to detect the most vascularized area, after which at least five microphotographs at high (200×) magnification of the mucosa were taken. The number of vessels/per field (expressed as mean vascular density) was measured using MetaMorph 7.0 videoimage analysis system (Molecular Devices, Downington, PA).

Experimental Design

Two D2R agonists were used: (1) quinpirole, which is the most widely used D2R agonist in in vivo and in vitro studies of D2R-mediated effects; (2) commercially available drug cabergoline, which has fewer side effects and a longer half-life in comparison with other commercially available D2R agonists [32]. Both compounds affect D2R centrally [33, 34] and peripherally [19, 35]. Dose regime for quinpirole and cabergoline treatment was designed based on published data on their effectiveness to prevent vascular permeability in vivo [19, 35]. Both compounds were dissolved in 0.9 % saline immediately before use.

Effect of D2R Agonist Quinpirole on Iodoacetamide-Induced UC in Rats

After iodoacetamide enema (the first day of experiment), rats were treated with quinpirole (1 mg/100 g, i.g.) or saline (0.8 ml/rat, i.g.) for 5 days starting from the second day of experiment [19]. Rats were euthanized on the seventh day. Clinical, macroscopic, and microscopic evaluation of UC onset and morphometric analysis of colonic microvasculature were performed.

Effect of D2R Agonist Quinpirole on Colitis in IL-10 KO Mice

IL-10 KO mice and WT littermates of 12 weeks old were divided into four groups: first—WT mice treated with saline ($n = 3$); second—WT mice treated with quinpirole ($n = 3$); third—IL-10 KO mice treated with saline ($n = 9$); fourth—IL-10 KO mice treated with quinpirole ($n = 9$). Quinpirole (1 mg/100 g, i.g.) or saline (0.1 ml/mouse, i.g.) was given for 13 days. Body weight and diarrhea were recorded on the first, fourth, eighth, and 14th day of the experiment. Mice were euthanized on the 14th day. At autopsy, the entire colon from anus to cecum and the spleen were carefully removed. Colon was opened longitudinally, rinsed with saline, and gently blotted with filter paper. The wet weights of colon and spleen were recorded and expressed as mg/10 g body weight. Subsequently, colonic segment was cut longitudinally: one half was snap-frozen in liquid nitrogen for further measurement of MPO activity and the second half was used for histologic evaluation of colonic lesions. All experiments were repeated at least two times, and data were pooled.

The Effectiveness of Cabergoline to Improve Signs of Experimental UC in Rats

Cabergoline is a synthetic ergoline 1-[(6-allylergolin-8ß-yl)-carbonyl]-1-[3-(dimethylamino) propyl]-3-ethylurea.

Doses of cabergoline were chosen based on a well-designed dose–effect study on a rat ovarian hyperstimulation model [35]. It was shown that cabergoline at 1 μg/100 g had no effect on vascular permeability, while at 5 μg/100 g, the drug slightly reduced VEGF-mediated vascular permeability without affecting angiogenesis. In the present study, cabergoline (1 or 5 μg/100 g, i.g.) or saline (0.8 ml/rat, i.g.) was given on the second and fifth days after iodoacetamide enema. Rats were euthanized on the seventh day. Clinical, macroscopic, and microscopic evaluations of colitis onset were performed.

Effect of D2R Activation on Vascular and Epithelial Permeability in Rats

The D2R agonist quinpirole (1 mg/100 g) or vehicle (0.8 ml saline) was administered by gavage 30 min before iodoacetamide enema. Vascular permeability was assessed in 0.5 and 1 h after iodoacetamide enema. Epithelial permeability was assessed in 1 h after iodoacetamide enema.

Statistical Analysis

Quantitative results are expressed as arithmetic mean ± SEM. The statistical significance was determined by the nonparametric Mann–Whitney *U* test or Student's *t* test, where appropriate. A p value of <0.05 was considered as a threshold for statistical significance in all analyses.

Results

Colonic Levels of TH, Dopamine Transporter DAT, and D2R in Experimental Models of IBD

As shown in Fig. 1a in rat colon during iodoacetamide-induced UC, colonic protein levels of the rate-limiting enzyme of dopamine synthesis TH were increased 1.3-fold at first 30 min, followed by a twofold ($p < 0.01$) decrease from 2 h that continued to diminish as the disease progressed. In 14 days, TH level was 3.8-fold lower versus control group ($p < 0.01$). Chronic IBD in IL-10 KO mice was associated with a twofold decrease in TH levels versus WT littermates (Fig. 1b).

Dopamine transporter DAT (a regulator of extracellular/intracellular dopamine balance) along with TH are markers of dopaminergic system and responsible for dopamine homeostasis. Strong dopamine transporter DAT-positive staining was found in colonic epithelial, endothelial cells, myenteric and submucosal neurons of control rats (Fig. 2b). Development of iodoacetamide-induced UC was associated with decreased DAT protein levels (Fig. 2a). At 2, 6 h, 7 and 14 days after iodoacetamide enema, DAT levels were 1.2-, 1.5-, 1.7- and 1.4-fold lower, respectively versus control rats. In inflamed colonic mucosa, DAT-positive staining was predominantly localized in surface colonocytes (Fig. 2b). Opposite to TH and DAT, protein levels of D2R in colonic mucosa were significantly increased in both models of IBD (Fig. 1c, d).

Effect of D2R Agonist Quinpirole on Iodoacetamide-Induced UC in Rats

There was a significant difference in the clinical signs of colitis (DAI) between the saline- and quinpirole-treated groups (Fig. 3a). At the time of killing, the saline-treated rats had 1.9-fold higher DAI than quinpirole-treated group ($p < 0.01$). Quinpirole markedly reduced the size of colonic lesions ($p < 0.01$ vs. saline) (Fig. 3b), colonic dilatation (an indicator of inflammation) ($p < 0.05$ vs. saline) (Fig. 3c), and ratio of colon wet weight/100 g of body weight ($p < 0.05$ vs. saline) (Fig. 3d) in rats with iodoacetamide-induced UC. Histologic evaluation confirmed our macroscopic observation, e.g., rats treated with quinpirole had smaller colonic ulcers, with minimal inflammation, while rats treated with saline had extensive ulcers surrounded by acute and chronic inflammatory cells, and no or minimal mucosal regeneration (Fig. 3e).

Effect of D2R Agonist Quinpirole on Colitis in IL-10 KO Mice

IL-10 KO mice spontaneously developed a chronic IBD, with incidence of 100 % by 12 weeks of age [36]. We did not see obvious signs of diarrhea in IL-10 KO mice treated with saline or quinpirole (data not shown), and there was no significant change in body weight (Fig. 4a). Nevertheless, 12-week-old IL-10 KO mice had 2.1-fold increase in colon wet weight ($p < 0.01$), 1.8-fold increase in spleen weight (marker of systemic inflammation), and 1.9-times higher colonic MPO activity (features of inflammation and disease severity) versus WT littermates ($p < 0.05$) (Fig. 4). Quinpirole administration for 13 days did not change colon wet weight in WT mice but significantly decreased it in IL-10 KO mice versus saline-treated IL-10 KO mice ($p < 0.05$) (Fig. 4b). The spleen weight was also reduced 1.5-fold in IL-10 KO mice by quinpirole treatment ($p < 0.001$) (Fig. 4c). MPO activity was decreased 1.3-fold in quinpirole-treated IL-10 KO mice, but this difference did not reach statistical significance ($p = 0.08$) (Fig. 4d). Histologic analysis of slides demonstrated that there was no significant difference between degree of inflammation in saline- and quinpirole-treated IL-10 KO mice.

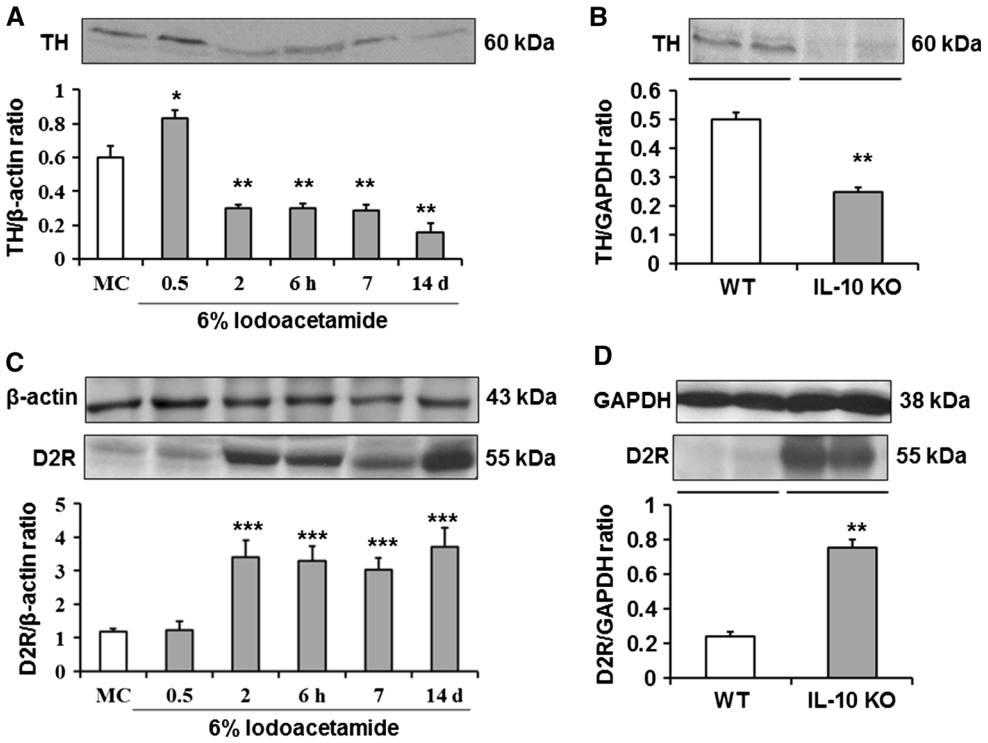

Fig. 1 Time-dependent changes in TH and D2R protein levels during iodoacetamide-induced colitis in rats (**a**, **c**) and spontaneously developed colitis in IL-10 KO mice (**b**, **d**). TH (**a**, **b**) and D2R (**c**, **d**) protein levels in colonic tissue were determined by Western blot. GAPDH or β-actin levels were used as loading controls. Assays were repeated 3 times with highly reproducible results using protein from 3 different animals/group. ** $p < 0.01$; *** $p < 0.001$ vs. MC (1% methylcellulose-vehicle)-treated rats (**a**, **c**) or WT mice (**b**, **d**)

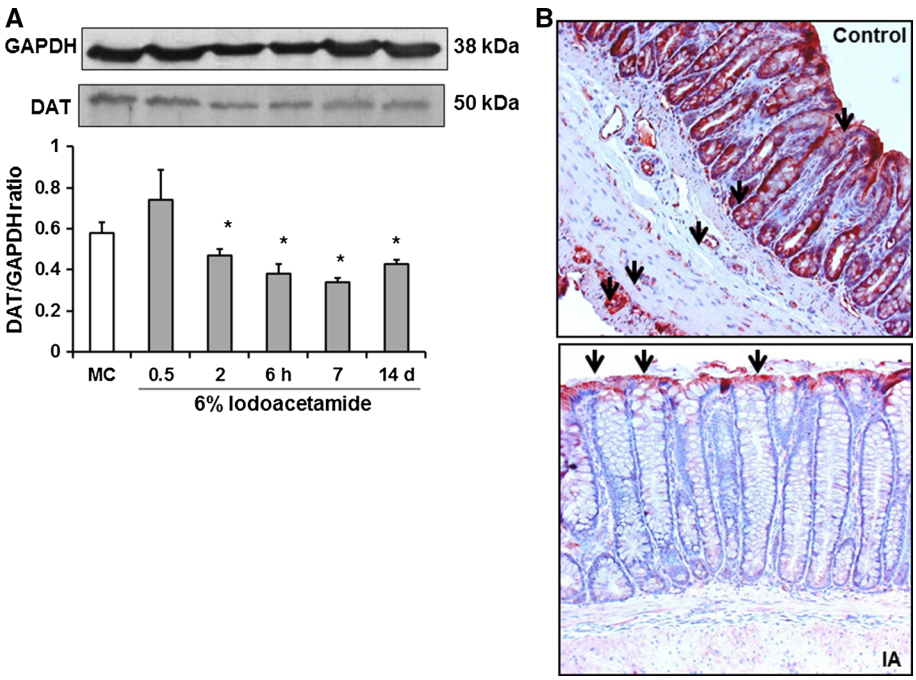

Fig. 2 Time-dependent changes in dopamine transporter DAT protein levels during iodoacetamide-induced colitis in rats. **a** DAT protein levels in colonic tissue were determined by Western blot. GAPDH levels were used as loading controls. Assays were repeated three times with highly reproducible results using protein from three different animals/groups. *$p < 0.05$ versus MC (1 % methylcellulose vehicle)-treated rats; **b** immunohistochemical localization of DAT in normal and inflamed colonic mucosa. (*Control*) DAT-positive staining in normal colon was localized to epithelial, endothelial cells, neurons of myenteric and submucosal plexus (*arrow*). (*IA*) Damaged colonic mucosa (7 days after iodoacetamide enema) had decreased DAT staining; DAT-positive staining was predominantly localized in surface colonocytes

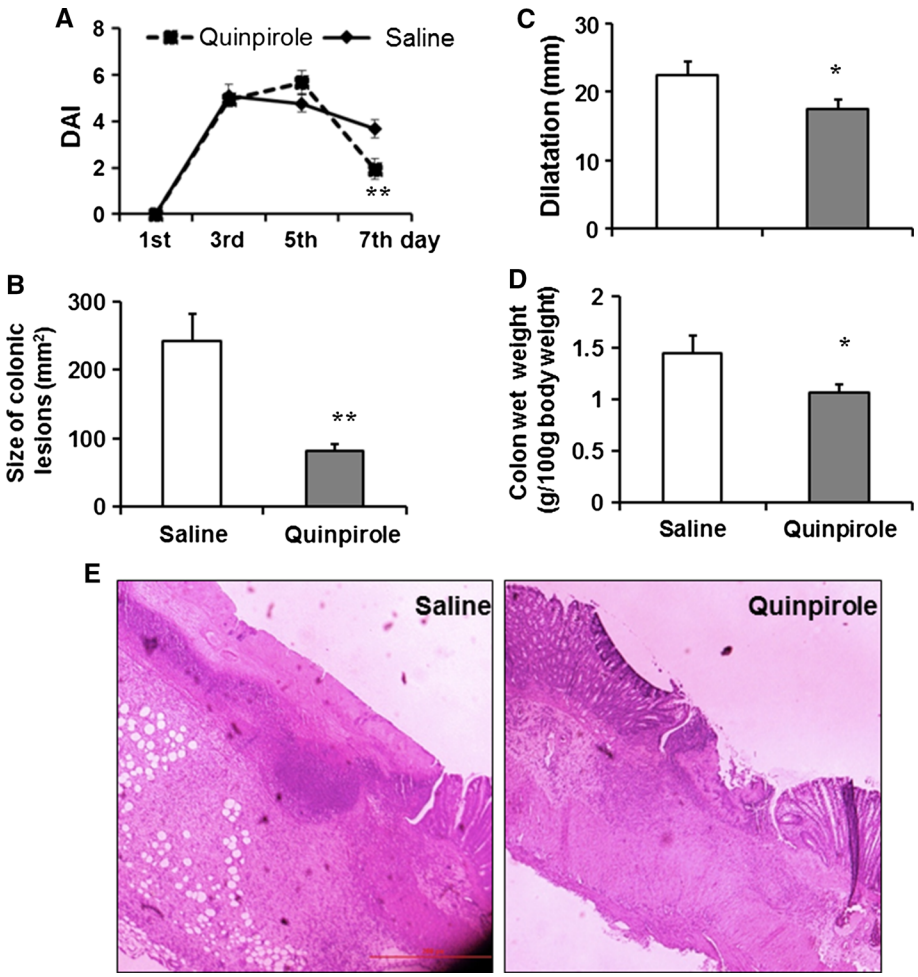

Fig. 3 Treatment with D2R agonist quinpirole significantly attenuated iodoacetamide-induced morphologic features of colitis in rats. **a** Disease activity index (DAI) and **b**–**d** macroscopic changes in colonic mucosa of saline versus quinpirole-treated rats. Results were expressed as mean ± SEM; $n = 10$ rats/group. *$p < 0.05$; **$p < 0.01$. **e** Light microscopy of the effect of quinpirole on histologic changes in the colon during iodoacetamide-induced colitis in rats (H&E staining, 20×). Colon from rats treated with saline after iodoacetamide had extensive ulcers surrounded by acute and chronic inflammatory cells, and no or minimal mucosal regeneration. Colon from rats treated with quinpirole after iodoacetamide had smaller colonic ulcers, with minimal inflammation

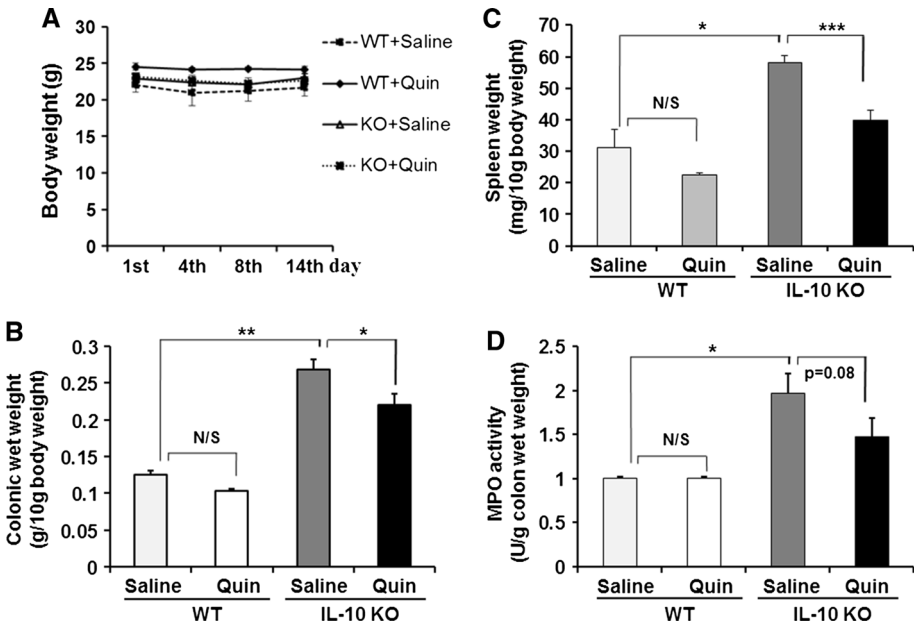

Fig. 4 Treatment with D2R agonist quinpirole (Quin) decreased disease severity in 12-week-old IL-10 KO mice versus mice treated with saline. **a** Mean body weights. **b** Quantitative measurements of colon and **c** spleen wet weight. **d** Quantitative measurements of MPO activity in colonic tissue. Results were expressed as mean ± SEM; $n = 9$ mice/group. *$p < 0.05$; **$p < 0.01$; ***$p < 0.001$

Effect of Quinpirole Treatment on Blood Vessel Density in the Colonic Mucosa During Iodoacetamide-Induced UC in Rats

We used immunohistochemistry with staining for anti-Von Willebrand factor as a highly selective endothelial cells marker for the angiogenesis assessment. Despite the marked differences in morphologic signs of iodoacetamide-induced UC after quinpirole treatment, there were no significant changes in blood vessel density in the ulcer base between saline-treated group (8 ± 2 vessels/per field) and the quinpirole-treated group (9 ± 1 vessels/per field).

The Role of D2R in Vascular and Epithelial Permeability in Pathogenesis of Experimental UC

Development of iodoacetamide-induced UC is characterized by increase in colonic vascular permeability as early as 15 min after iodoacetamide enema with maximal effect in 1–2 h [30]. Pretreatment with quinpirole 30 min before iodoacetamide enema markedly attenuated Evans blue extravasations in colonic mucosa, indicating a reduction in iodoacetamide-induced increased vascular permeability (Fig. 5a). The effect of quinpirole was sustained and detected in 0.5 h ($p = 0.06$) and 1 h ($p = 0.03$) after iodoacetamide administration. Unlike colonic vascular permeability, quinpirole did not affect iodoacetamide-induced increase in colonic epithelial permeability (Fig. 5b). Quinpirole-induced downregulation of colonic vascular permeability was associated with decreased phosphorylation (activation) c-Src and Akt, two main signaling molecules responsible for VEGF-induced vascular permeability [37, 38], while levels of total proteins c-Src and Akt were unchanged (Fig. 5c).

The Effect of Cabergoline on Iodoacetamide-Induced UC in Rats

To further confirm the effectiveness of D2R activation for IBD treatment via prevention of vascular permeability and to consider possible clinical implications, we treated rats

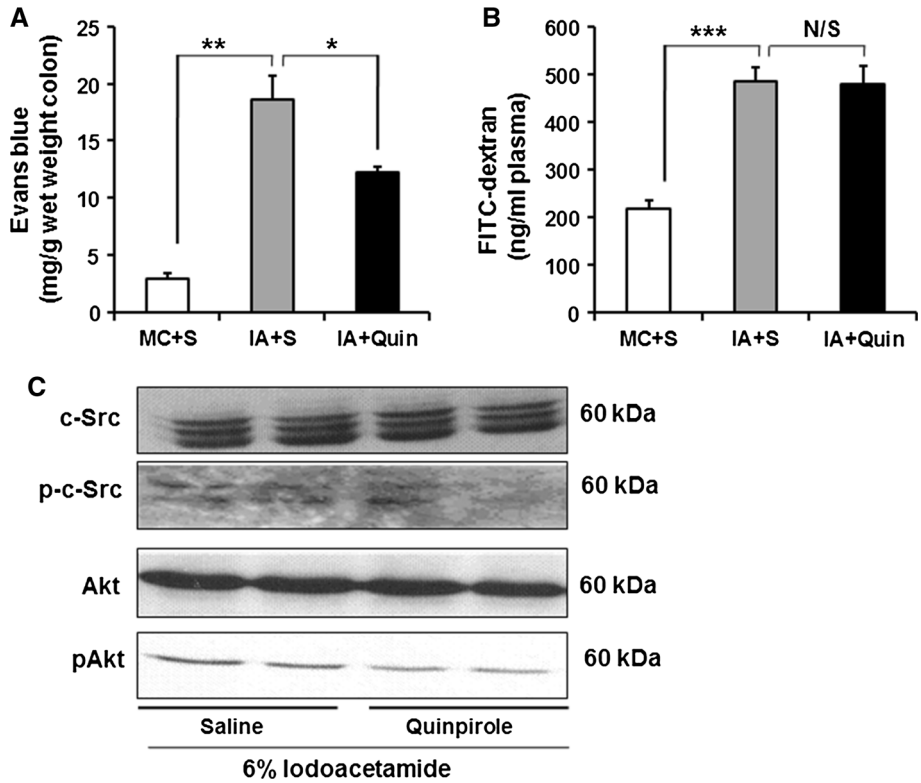

Fig. 5 Pretreatment with D2R agonist quinpirole (Quin) decreased vascular permeability but did not affect epithelial permeability in colonic mucosa during iodoacetamide-induced colitis in rats. **a** Quantitative measurements of vascular permeability by extraction of extravasated Evans blue in colonic mucosa. **b** Quantitative measurements of colonic epithelial permeability by measurement of serum concentration of orally administered FITC–dextran. **c** Representative Western blots of altered activation of c-Src and Akt signal pathways in rat colonic tissue during 6 % iodoacetamide-induced colitis. Results were expressed as mean ± SEM; $n = 5$ rats/group. *$p < 0.05$; **$p < 0.01$; ***$p < 0.001$ versus saline (S)-treated groups (MC-1 % methylcellulose vehicle; IA—6 % iodoacetamide)

with iodoacetamide-induced UC with commercially available D2R agonist cabergoline. In our study, treatment with cabergoline at 1 μg/100 g (no effect on vascular permeability [35]) had no significant influence on clinical and macroscopic signs of iodoacetamide-induced UC in rats (Fig. 6), while 5 μg/100 g of cabergoline significantly improved clinical (DAI) and morphologic signs of experimental UC. Mean DAI in cabergoline-treated group was 1.4- ($p < 0.05$), 1.6- ($p < 0.01$) and 1.5-fold ($p < 0.05$) lower versus saline-treated group, respectively, on the third, fifth, and seventh day of experiment (Fig. 6a). Cabergoline-treated group had 6 % mortality (1/16 rats) versus 17 % (3/17 rats) in saline group. These changes were also reflected in the size of macroscopic (Fig. 6b–d) and microscopic (Fig. 6e) colonic lesions. As shown in Fig. 6b–d, 5 μg/100 g of cabergoline markedly reduced the size of colonic lesions ($p < 0.05$ vs. saline), colonic dilatation ($p < 0.05$ vs. saline), and ratio of colon wet weight/100 g of body weight ($p < 0.05$ vs. saline) in rats with iodoacetamide-induced UC.

Discussion

The present study demonstrated for the first time a protective role of dopamine and D2R in the pathogenesis of IBD. In two animal models of IBD, acute and chronic stages of disease were accompanied by diminished synthesis of dopamine in the colonic mucosa. Agonists of D2R markedly attenuated the features of chemically induced UC in rats and spontaneously developing colitis in IL-10 KO mice. Mechanistic study in rats with chemically induced UC revealed that D2R agonists were able to reduce colonic vascular permeability. These findings provide compelling evidence for the importance of dopaminergic system in the pathogenesis of IBD and might have translational significance for new therapeutic considerations. More studies are needed to design treatment protocols, taking into account stage of disease and pharmacokinetic of commercially available D2R agonists.

Dopamine synthesis depends on the rate of conversion by TH of amino acid tyrosine into the immediate precursor

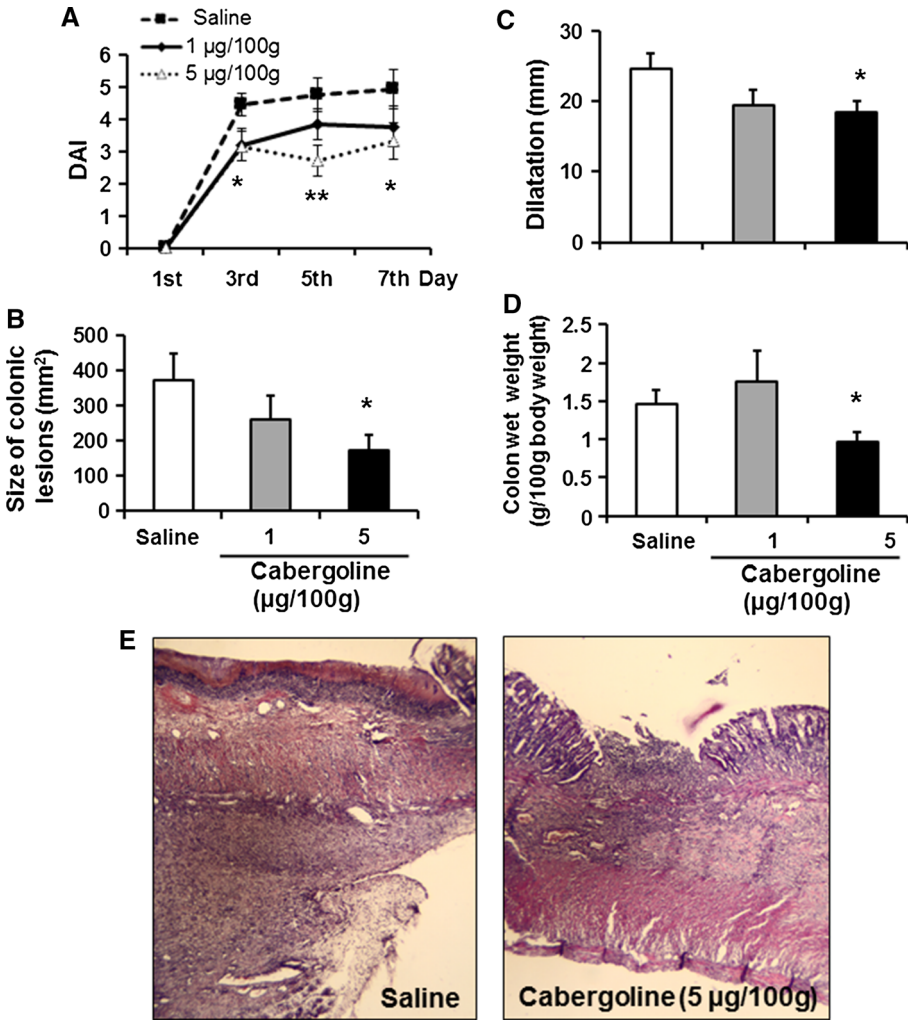

Fig. 6 Treatment with commercially available D2R agonist cabergoline in dose of 5 μg/100 g (which reduces vascular permeability), but not at 1 μg/100 g (no effect on vascular permeability) significantly attenuated iodoacetamide-induced morphologic features of colitis in rats. **a** Disease activity index (DAI) and **b–d** macroscopic changes in colonic mucosa of saline versus cabergoline-treated rats (1 or 5 μg/100 g, per os). **e** Light microscopy of the effect of cabergoline (5 μg/100 g, per os) on histologic changes in the colon during iodoacetamide-induced colitis in rats (H&E staining, ×4). Colon from rats treated with saline and cabergoline on the seventh day after iodoacetamide enema. Results were expressed as mean ± SEM; $n = 16$–17 rats/group. *$p < 0.05$; **$p < 0.01$ versus saline-treated group

of dopamine L-3,4-dihydroxyphenylalanine (L-DOPA) [39]. Studies in sympathectomized animals along with detection of non-neuronal TH-positive cells and measuring levels of dopamine metabolite 3,4-dihydroxyphenylacetic acid (DOPAC) revealed that dopamine activity on the periphery is far beyond simple precursor of norepinephrine/epinephrine synthesis [40–43]. Dopamine effects are mediated through its interaction with five subtypes of dopamine receptors, which can be grouped in two families: D1-like family (D1, D5) and D2-like family (D2, D3, D4) [39]. Expression of D2R was detected in adult [19, 44] as well as progenitor [45] endothelial cells and was found predominantly in the distal colon versus other parts of the gut [46]. In endothelial cells, D2R is a negative regulator of VEGF–VEGFR2-mediated increase in vascular permeability and pathologic blood vessels remodeling [19, 21, 23, 45].

In our study with models of chemically induced UC in rats as well as spontaneously developed colitis in IL-10 KO mice, the decrease in colonic levels of TH was correlated with disease progression. Along with TH, the expression of dopamine transporter DAT was also decreased. The simultaneous decrease in TH and DAT levels represents augmentation in dopamine synthesis and reuptake, respectively, thereby reducing dopaminergic tone in colonic mucosa during IBD. We showed the wide distribution of DAT in normal colonic tissue, namely in epithelial, endothelial cells, as well as enteric neurons. Previously, we described dopamine binding sites in gastric and duodenal mucosa and muscularis propria [47], while the expression of DAT in epithelial cells of stomach, namely parietal cells, was reported by Mezey et al. [43]. Tian et al. [48] showed the co-expression of TH and DAT in epithelial cells of stomach, duodenum, and colon. Profound expression of DAT on epithelial cells reconfirms the significance of food [49] and possibly microbiota metabolites [50] as an important source of endogenous dopamine. Development of inflammation during experimental IBD was associated with significant DAT downregulation that might be responsible for decreasing of luminal dopamine uptake and, as a result, dopamine deficiency during IBD. In line with our findings, Magro et al. [24] showed markedly lower levels of dopamine and significant reduction in dopamine/L-DOPA tissue ratio (marker of decrease L-amino acid decarboxylase activity) in the inflamed mucosa of CD and UC patients. The expression of DAT in endothelial cells was not reported before, though uptake of dopamine and its metabolism by pulmonary endothelial cells has been shown [51].

Unlike levels of TH and DAT, colonic levels of D2R were significantly increased in both models of IBD. Upregulation of D2R might be a compensatory reaction for decreased local dopaminergic tone and supports the importance of D2R in feedback regulation of dopamine biosynthesis and reuptake showed in experiments on D2R-KO mice [52] and confirmed in the Parkinson's disease rat model [53]. On the other hand, an increased expression of D2R, similar to expression pattern of VEGFR2, was found in endothelial cells lining newly formed blood vessels in mice injected with adenoviral vector (VEGF) [19], likely due to excessive levels of VEGF. In our previous study [54], we also showed the increased levels of VEGF as well as VEGFR2 in both models of IBD.

Our mechanistic study further confirmed the important role of dopamine/D2R pathway in IBD pathogenesis. Treatment of both rats and mice with D2R agonist quinpirole significantly decreased morphologic signs of IBD. We found less profound effect in IL-10 KO mice versus chemically induced UC in rats, and this might be related to the insufficient period of treatment for the prevention of this chronic disease in mice. Treatment of rats started at early time points of disease development (24 h after iodoacetamide enema, acute colitis), while at the beginning of the treatment, all IL-10 KO mice already had well-developed chronic IBD. Moreover, D2R activation decreased vascular permeability, which is a major contributor in acute inflammation. D2R-induced inhibition of colonic vascular permeability was associated with decreased activation/phosphorylation of c-Src and Akt that mediate VEGF/VEGFR2-induced vascular permeability and whose sustained activation was shown in acute and chronic models of IBD [54]. Further studies are warranted to compare the usefulness of D2R agonists in chronic and acute disease.

In our study, the D2R agonist did not have a direct effect on colonic epithelial permeability, supporting the primary role of endothelial layer restitution for the successful treatment outcome in IBD [30]. The commercially available D2R agonist cabergoline which showed effectiveness in prevention of increased vascular permeability in patients with ovarian hyperstimulation syndrome [55], in small doses, activates D2R and reduces VEGF-mediated vascular permeability without affecting angiogenesis [35], improved clinical and morphologic signs of experimental UC in our study.

In the present study, we used two D2R agonists (quinpirole and cabergoline), both of which are able to cross blood brain barrier. Thus, we cannot exclude the role of central D2R in beneficial effect of D2R agonists on healing of colonic lesions. Based on our previous studies, both central and peripheral dopamine play a mechanistic role in duodenal ulceration [56, 57]. So far, no direct data on the role of central dopamine in IBD pathogenesis are available, except evidence that patients with Parkinson disease have elevated colonic level of pro-inflammatory cytokines [58] and increased intestinal permeability [59, 60], which are hallmarks of IBD pathogenesis.

Furthermore, the importance of central dopamine in intestinal mucosal integrity was confirmed by Ray et al. [61, 62]. They showed that microinjection of dopamine or D2R agonist bromocriptine in amygdala dose-dependently attenuated stress-induced gastric ulcer formation in rats. Besides nervous system, immune cells are additional source of dopamine. Moreover, expression of D2R was found in the CD4+ T cells, B cells, NK cells, and, in lesser extent, in neutrophils and dendritic cells [63, 64]. Study on the resting normal-human T cells showed that D2R agonist was able to upregulate IL-10 expression [64]. Taking into account that IL-10 is the central anti-inflammatory cytokine in IBD pathogenesis, the described in our study beneficial effect of D2R agonist might also be explained by upregulation of IL-10 levels. Described above justifies the possible role of central dopamine and immune cells regulation by D2Rs in IBD pathogenesis, which needs further investigation.

The successful treatment of two patients with severe refractory CD [65] and UC [66] with dextroamphetamine sulfate, which produces its effect through indirect release of dopamine and edema prevention [67], further supports our proposal on the new role of dopamine in IBD pathogenesis.

Acknowledgments The present study was supported by a Department of Veterans Affairs, Veterans Health Administration Merit Review Grant VAMR0710-580 and VAMR0810-877 to Zs. Sandor and S. Szabo and by U.S. Civilian Research & Development Foundation (CRDF) CREST II Junior Scientist Research Collaboration Program 09DP036-05 and the Ministry of Education and Science of Ukraine Grant 15BF036-01 to G. Tolstanova

Conflict of interest None.

References

1. Burisch J, Jess T, Martinato M, et al. The burden of inflammatory bowel disease in Europe. *J Crohns Colitis*. 2013;7:322–337.
2. Rocchi A, Benchimol EI, Bernstein CN, et al. Inflammatory bowel disease: a Canadian burden of illness review. *Can J Gastroenterol*. 2012;26:811–817.
3. Ording AG, Horváth-Puhó E, Erichsen R, et al. Five-year mortality in colorectal cancer patients with ulcerative colitis or Crohn's disease: a nationwide population-based cohort study. *Inflamm Bowel Dis*. 2013;19:800–805.
4. Brahme F, Lindstrom C. A comparative radiographic and pathological study of intestinal vaso-architecture in Crohn's disease and in ulcerative colitis. *Gut*. 1970;11:928–940.
5. Chidlow JH Jr, Langston W, Greer JJM, et al. Differential angiogenic regulation of experimental colitis. *Am J Pathol*. 2006;169:2014–2030.
6. Danese S, Sans M, Motte CDL, et al. Angiogenesis as a novel component of inflammatory bowel disease pathogenesis. *Gastroeneterology*. 2006;130:2060–2073.
7. Foitzik T, Kruschewski M, Kroesen A, et al. Does microcirculation play a role in the pathogenesis of inflammatory bowel diseases? Answers from intravital microscopic studies in animal models. *Int J Colorectal Dis*. 1999;14:29–34.
8. Hatoum OA, Miura H, Binion DG. The vascular contribution in the pathogenesis of inflammatory bowel disease. *Am J Physiol Heart Circ Physiol*. 2003;285:1791–1796.
9. Spalinger J, Patriquin H, Miron MC, et al. Doppler US in patients with Crohn disease: vessel density in the diseased bowel reflects disease activity. *Radiology*. 2000;217:787–791.
10. Schinzari F, Armuzzi A, De Pascalis B, et al. Tumor necrosis factor-alpha antagonism improves endothelial dysfunction in patients with Crohn's disease. *Clin Pharmacol Ther*. 2008;83:70–76.
11. Tolstanova G, Khomenko T, Deng X, et al. Neutralizing anti-vascular endothelial growth factor (VEGF) antibody reduces severity of experimental ulcerative colitis in rats: direct evidence for the pathogenic role of VEGF. *J Pharmacol Exp Ther*. 2009;328:749–757.
12. Chidlow JH Jr, Glawe JD, Pattilllo CB, et al. $VEGF_{164}$ isoform specific regulation of T-cell-dependent experimental colitis in mice. *Inflamm Bowel Dis*. 2011;17:1501–1512.
13. Jerkic M, Peter M, Ardelean D, et al. Dextran sulfate sodium leads to chronic colitis and pathological angiogenesis in Endoglin heterozygous mice. *Inflamm Bowel Dis*. 2010;16:1859–1870.
14. Scaldaferri F, Vetrano S, Sans M, et al. VEGF-A links angiogenesis and inflammation in inflammatory bowel disease pathogenesis. *Gastroenterology*. 2009;136:585–595.
15. Plevy S, Silverberg MS, Lockton S, et al. Combined Serological, Genetic, and Inflammatory Markers Differentiate Non-IBD, Crohn's Disease, and Ulcerative Colitis Patients. *Inflamm Bowel Dis*. 2013;19:1139–1148.
16. Coriat R, Mir O, Leblanc S, et al. Feasibility of anti-VEGF agent bevacizumab in patients with Crohn's disease. *Inflamm Bowel Dis*. 2011;17:1632.
17. Shaughnessy AF. Monoclonal antibodies: magic bullets with a hefty price tag. *BMJ*. 2012;345:8346.
18. Loriot Y, Boudou-Rouquette P, Billemont B, et al. Acute exacerbation of hemorrhagic rectocolitis during antiangiogenic therapy with sunitinib and sorafenib. *Ann Oncol*. 2008;19:1975.
19. Basu S, Nagy JA, Pal S, et al. The neurotransmitter dopamine inhibits angiogenesis induced by vascular permeability factor/vascular endothelial growth factor. *Nat Med*. 2001;7:569–574.
20. Sarkar C, Chakroborty D, Chowdhury UR, et al. Dopamine increases the efficacy of anticancer drugs in breast and colon cancer preclinical models. *Clin Cancer Res*. 2008;14:2502–2510.
21. Basu S, Sarkar C, Chakroborty D, et al. Ablation of peripheral dopaminergic nerves stimulates malignant tumor growth by inducing vascular permeability factor/vascular endothelial growth factor-mediated angiogenesis. *Cancer Res*. 2004;64:5551–5555.
22. Bhattacharya R, Sinha S, Yang SP, et al. The neurotransmitter dopamine modulates vascular permeability in the endothelium. *J Mol Signal*. 2008;3:14.
23. Chakroborty D, Sarkar C, Yu H, et al. Dopamine stabilizes tumor blood vessels by up-regulating angiopoietin 1 expression in pericytes and Kruppel-like factor-2 expression in tumor endothelial cells. *Proc Natl Acad Sci USA*. 2011;108:20730–20735.
24. Magro F, Vieira-Coelho MA, Fraga S, et al. Impaired synthesis or cellular storage of norepinephrine, dopamine, and 5-hydroxytryptamine in human inflammatory bowel disease. *Dig Dis Sci*. 2002;47:216–224.
25. Magro F, Fraga S, Ribeiro T, et al. Decreased availability of intestinal dopamine in transmural colitis may relate to inhibitory effects of interferon-gamma upon L-DOPA uptake. *Acta Physiol Scand*. 2004;180:379–386.
26. Magro F, Cunha E, Araujo F, et al. Dopamine D2 receptor polymorphisms in inflammatory bowel disease and the refractory response to treatment. *Dig Dis Sci*. 2006;51:2039–2044.
27. Satoh H, Sato F, Takami K, et al. New ulcerative colitis model induced by SH blockers in rats and the effects of antiinflammatory drugs on the colitis. *Jpn J Pharmacol*. 1997;73:299–309.

28. Castaneda FE, Walia B, Vijay-Kumar M, et al. Targeted deletion of metalloproteinase 9 attenuates experimental colitis in mice: central role of epithelial-derived MMP. *Gastroenterology*. 2005;129:1991–2008.
29. Patterson CE, Rhoades RA, Garcia JG. Evans blue dye as a marker of albumin clearance in cultured endothelial monolayer and isolated lung. *J Appl Physiol*. 1992;72:865–873.
30. Tolstanova G, Deng X, French SW, et al. Early endothelial damage and increased colonic vascular permeability in the development of experimental ulcerative colitis in rats and mice. *Lab Invest*. 2012;92:9–21.
31. Khomenko T, Szabo S, Deng X, et al. Suppression of early growth response factor-1 with egr-1 antisense oligodeoxynucleotide aggravates experimental duodenal ulcers. *Am J Physiol Gastrointest Liver Physiol*. 2006;290:G1211–G1218.
32. Webster J. A comparative review of the tolerability profiles of dopamine agonists in the treatment of hyperprolactinaemia and inhibition of lactation. *Drug Saf*. 1996;14:228–238.
33. Benedetti MS, Dostert P, Barone D, et al. In vivo interaction of cabergoline with rat brain dopamine receptors labelled with [3H]N-n-propylnorapomorphine. *Eur J Pharmacol*. 1990;187:399–408.
34. Lahlou S. Involvement of spinal dopamine receptors in mediation of the hypotensive and bradycardic effects of systemic quinpirole in anaesthetised rats. *Eur J Pharmacol*. 1998;353:227–237.
35. Gomez R, Gonzalez-Izquierdo M, Zimmermann RC, et al. Low-dose dopamine agonist administration blocks vascular endothelial growth factor (VEGF)-mediated vascular hyperpermeability without altering VEGF receptor 2-dependent luteal angiogenesis in a rat ovarian hyperstimulation model. *Endocrinology*. 2006;147:5400–5411.
36. Berg DJ, Davidson N, Kuhn R, et al. Enterocolitis and colon cancer in interleukin-10-deficient mice are associated with aberrant cytokine production and $CD4^+$ TH1-like responses. *J Clin Invest*. 1996;98:1010–1020.
37. Gavard J, Gutkind JS. VEGF controls endothelial-cell permeability by promoting the β-arrestin-dependent endocytosis of VE-cadherin. *Nat Cell Biol*. 2006;8:1223–1234.
38. Kilic E, Kilic U, Wang Y, et al. The phosphatidylinositol-3 kinase/Akt pathway mediates VEGF's neuroprotective activity and induces blood brain barrier permeability after focal cerebral ischemia. *FASEB J*. 2006;20:1185–1187.
39. Beaulieu JM, Gainetdinov RR. The physiology, signaling, and pharmacology of dopamine receptors. *Pharmacol Rev*. 2011;63:182–217.
40. Eaker EY, Bixler GB, Dunn AJ, et al. Dopamine and norepinephrine in the gastrointestinal tract of mice and the effects of neurotoxins. *J Pharmacol Exp Ther*. 1988;244:438–442.
41. Eisenhofer G, Aneman A, Friberg P, et al. Substantial production of dopamine in the human gastrointestinal tract. *J Clin Endocrinol Metab*. 1997;82:3864–3871.
42. Eldrup E, Richter EA, Christensen NJ. DOPA, norepinephrine, and dopamine in rat tissues: no effect of sympathectomy on muscle DOPA. *Am J Physiol*. 1989;256:284–287.
43. Mezey E, Eisenhofer G, Hansson S, et al. Non-neuronal dopamine in the gastrointestinal system. *Clin Exp Pharmacol Physiol Suppl*. 1999;26:14–22.
44. Kim HJ, Koh PO, Kang SS, et al. The localization of dopamine D2 receptor mRNA in the human placenta and the anti-angiogenic effect of apomorphine in the chorioallantoic membrane. *Life Sci*. 2001;68:1031–1040.
45. Sinha S, Vohra PK, Bhattacharya R, et al. Dopamine regulates phosphorylation of VEGF receptor 2 by engaging Src-homology-2-domain-containing protein tyrosine phosphatase 2. *J Cell Sci*. 2009;122:3385–3392.
46. Li ZS, Schmauss C, Cuenca A, et al. Physiological modulation of intestinal motility by enteric dopaminergic neurons and the D2 receptor: analysis of dopamine receptor expression, location, development, and function in wild-type and knock-out mice. *J Neurosci*. 2006;26:2798–2807.
47. Szabo S, Sandrock AW, Nafradi J, et al. Dopamine and dopamine receptors in the gut: their possible role in duodenal ulceration. In: Kawasaki M, et al., eds. *Advances in dopamine research*. Oxford: Pergamon Press; 1982:165–170.
48. Tian YM, Chen X, Luo DZ, et al. Alteration of dopaminergic markers in gastrointestinal tract of different rodent models of Parkinson's disease. *Neuroscience*. 2008;153:634–644.
49. Eldrup E, Richter EA. DOPA, dopamine, and DOPAC concentrations in the rat gastrointestinal tract decrease during fasting. *Am J Physiol Endocrinol Metab*. 2000;279:815–822.
50. Asano Y, Hiramoto T, Nishino R, et al. Critical role of gut microbiota in the production of biologically active, free catecholamines in the gut lumen of mice. *Am J Physiol Gastrointest Liver Physiol*. 2012;303:1288–1295.
51. Bryan-Lluka LJ, O'Donnell SR. Dopamine and adrenaline, but not isoprenaline, are substrates for uptake and metabolism in isolated perfused lungs of rats. *Naunyn Schmiedebergs Arch Pharmacol*. 1992;346:20–26.
52. Tarnawski A, Coron E, Mosnier JF, et al. In-vivo detection by confocal endomicroscopy of two distinct structural abnormalities in angioarchitecture and increased VP in colonic mucosa of patients with IBD in remission: mechanistic implications. *Gastroenterology*. 2009;136:112.
53. Colucci M, Cervio M, Faniglione M, et al. Intestinal dysmotility and enteric neurochemical changes in a Parkinson's disease rat model. *Auton Neurosci*. 2012;169:77–86.
54. Tolstanova G, Khomenko T, Deng X, et al. New molecular mechanisms of the unexpectedly complex role of VEGF in ulcerative colitis. *Biochem Biophys Res Commun*. 2010;399:613–616.
55. Alvarez C, Martí-Bonmatí L, Novella-Maestre E, et al. Dopamine agonist cabergoline reduces hemoconcentration and ascites in hyperstimulated women undergoing assisted reproduction. *J Clin Endocrinol Metab*. 2007;92:2931–2937.
56. Szabo S, Horner HC, Maull H, et al. Biochemical changes in tissue catecholamines and serotonin in duodenal ulceration caused by cysteamine or propionitrile in the rat. *J Pharmacol Exp Ther*. 1987;240:871–878.
57. Horner HC, Szabo S. Differential effect of changing central and peripheral catecholamine levels in cysteamine-induced duodenal ulcer in the rat. *Life Sci*. 1981;29:2437–2443.
58. Devos D, Lebouvier T, Lardeux B, et al. Colonic inflammation in Parkinson's disease. *Neurobiol Dis*. 2013;50:42–48.
59. Forsyth Christopher B, Kathleen M, et al. Increased intestinal permeability correlates with sigmoid mucosa alpha-synuclein staining and endotoxin exposure markers in early Parkinson's disease. *PLoS One*. 2011;6:28032.
60. Salat-Foix D, Tran K, Ranawaya R, et al. Increased intestinal permeability and Parkinson disease patients: chicken or egg? *Can J Neurol Sci*. 2012;39:185–188.
61. Ray A, Henke PG, Sullivan RM. Effects of intra-amygdalar dopamine agonists and antagonists on gastric stress lesions in rats. *Neurosci Lett*. 1988;84:302–306.
62. Ray A, Henke PG. The basolateral amygdala, dopamine and gastric stress ulcer formation in rats. *Brain Res*. 1991;558:335–338.
63. McKenna F, McLaughlin PJ, Lewis BJ, et al. Dopamine receptor expression on human T- and B-lymphocytes, monocytes, neutrophils, eosinophils and NK cells: a flow cytometric study. *J Neuroimmunol*. 2002;132:34–40.
64. Besser MJ, Ganor Y, Levite M. Dopamine by itself activates either D2, D3 or D1/D5 dopaminergic receptors in normal human T-cells and triggers the selective secretion of either IL-10, TNFalpha or both. *J Neuroimmunol*. 2005;169:161–171.

65. Check JH, Katsoff B, Cohen R. Novel highly effective medical treatment of severe treatment refractory Crohn's disease using sympathomimetic amines: case report. *Inflamm Bowel Dis*. 2010;16:1999–2000.
66. Check JH, Katsoff B, Cohen R. Case report showing that a woman with ulcerative colitis refractory to standard therapy responded well to the sympathomimetic amine dextroamphetamine sulfate. *Inflamm Bowel Dis*. 2011;17:870–871.
67. Check JH, Amadi C, Kaplan H, Katsoff D. The treatment of idiopathic edema, a cause of chronic pelvic pain in women: effectively controlled chronic refractory urticaria–case reports. *Clin Exp Obstet Gynecol*. 2006;33:183–184.